An Improved Instrumental Variable Method for Industrial Robot Model Identification

M. Brunot[a,b,*], A. Janot[a], P.C. Young[c,d], F. Carrillo[b]

[a] *ONERA, 2 Avenue Edouard Belin, 31055 Toulouse, France*
[b] *LGP ENI Tarbes, 47 avenue d'Azereix, BP 1629, 65016 Tarbes, France*
[c] *Systems and Control Group, Lancaster Environment Centre, Lancaster University, UK*
[d] *Integrated Catchment Assessment and Management Centre, Australian National University College of Medicine, Biology & Environment, Canberra, ACT*

Abstract

Industrial robots are electro-mechanical systems with double integrator behaviour, necessitating operation and model identification under closed-loop control conditions. The Inverse Dynamic Identification Model (IDIM) is a mechanical model based on Newton's laws that has the advantage of being linear with respect to the parameters. Existing Instrumental Variable (IDIM-IV) estimation provides a robust solution to this estimation problem and the paper introduces an improved IDIM-PIV method that takes account of the additive noise characteristics by adding prefilters that provide lower variance estimates of the IDIM parameters. Inspired by the prefiltering approach used in optimal Refined Instrumental Variable (RIV) estimation, the IDIM-PIV method identifies the nonlinear physical model of the robot, as well as the noise model resulting from the feedback control system. It also has the advantage of providing a systematic prefiltering process, in contrast to that required for the previous IDIM-IV method. The issue of an unknown controller is also considered and resolved using existing parametric identification. The evaluation of the new estimation algorithms on a six degrees-of-freedom rigid robot shows that they improve statistical efficiency, with the controller either known or identified as an intrinsic part of the IDIM-PIV algorithm.

Keywords: refined instrumental variable, closed-loop system identification, robot identification, inverse dynamics, dynamic parameters, robot dynamics

*Corresponding author
Email address: Mathieu.Brunot@onera.fr (M. Brunot)

1. Introduction

Robots are mechanical systems that have a double integrator behaviour and they must be identified, therefore, while operating in closed-loop. Their direct and inverse dynamic models are formulated in continuous time and are calculated from Newton's laws or the Lagrange equations (Khalil and Dombre, 2004). The method based on the inverse dynamic identification model (IDIM) and least squares estimation (LS) is the standard procedure to identify the dynamic parameters of robots. This approach, termed IDIM-LS, has been successfully applied to identify the dynamic parameters of several prototypes and industrial robots (see (Khosla and Kanade, 1985), (Raucent et al., 1992), (Swevers et al., 1997), (Olsen et al., 2002), (Wu et al., 2008), (Calanca et al., 2011), (Briot and Gautier, 2015), among others). Good results can be obtained provided that an appropriate derivative bandpass filtering of the joint positions is used in order to calculate the joint velocities and accelerations. However, even with the guidelines for tuning the bandpass filtering given in (Gautier, 1997), the user can doubt whether the IDIM-LS estimates are consistent or not because robots are identified while they are operating in closed loop while it is known that the LS estimates are biased in this case (Van den Hof, 1998).

Other identification methods have been evaluated: the Total Least Squares method (Xi, 1995) and (Hollerbach and Nahvi, 1997); the Extended Kalman Filter (Gautier and Poignet, 2001) and (Kostic et al., 2004); the Set Membership Uncertainty (Ramdani and Poignet, 2005); an algorithm based on LMI tools in (Calafiore and Indri, 1999); a ML approach (Olsen et al., 2002), (Dolinskỳ and Čelikovskỳ, 2017); the closed-loop output error (Östring et al., 2003) and (Gautier et al., 2013a); a Bayesian approach (Ting et al., 2006); a method which estimates the nonlinear effects in the frequency domain (Wernholt and Gunnarsson, 2008); the Unscented Kalman Filter (Dellon and Matsuoka, 2009); an algorithm based on neural network (Soewandito et al., 2011). In (Calanca et al., 2011), the authors suggest to complete the IDIM-LS method with deeper statistical analyses; while in (Miranda-Colorado and Moreno-Valenzuela, 2017), the authors propose an improvement to the standard approach by using an algebraic technique for state estimation and a procedure based on the Semi-Definite Programming (Wensing et al., 2018). An overview of some of these methods is given by Wu et al. (2010). Al-

though all these techniques are of great interest, they do not really improve the IDIM-LS method, even when combined with the derivative bandpass filtering, because the LS estimates are still asymptotically biased. Also, the robustness against data filtering has not been studied; and some of these approaches have not been validated on a 6 DOF industrial robot. Except for the approach presented in (Gautier et al., 2013a), only the direct or inverse dynamic model is validated and the condition that the columns of the observation matrix are not correlated with the error terms is not addressed,, even though it is a critical condition to obtain consistent estimates, see e.g. (Young, 2011).

An approach able to provide consistent estimates while the system is identified in closed loop is the instrumental variables (IV) technique introduced by Reiersøl (Reiersøl, 1941). In the system identification community, IV methods have been studied extensively; see e.g. Young (1970, 1981, 2011) for continuous time systems; and Wong and Polak (1967); Rowe (1970); Jakeman and Young (1979); Söderström and Stoica (1983); Young (1976, 2011) for discrete time systems. One interesting feature of the optimal Refined IV approach to both continuous (RIVC) and discrete-time (RIV) model identification (Young, 2015) is the use of an optimal prefiltering process which takes into account the noise model and so provides statistically efficient estimates (i.e. with minimum variance). Furthermore, for systems identified in closed-loop, specific techniques are able to deal with an unknown controller: see e.g. Gilson et al. (2011); Young (2011). Although these methods are appealing, they were developed primarily for Linear Time Invariant (LTI) systems and so cannot be applied straightforwardly to complex, nonlinear robot systems. This may explain why there are few applications in robotics (see e.g. (Puthenpura and Sinha, 1986), (Yoshida et al., 1993) and (Xi, 1995)). A first attempt to bridge the gap between robotics and automatic control was made in (Janot et al., 2014a) where a generic IV approach relevant for the identification of rigid industrial robots was proposed. The set of instruments is the IDM constructed from simulated data calculated from the simulation of the DDM. The simulation of the direct dynamic model assumes the same reference trajectories and the same control structure for both the actual and the simulated robots and is based on the previous IV estimates. This algorithm, termed the IDIM-IV method, validates the inverse and direct dynamic models simultaneously, improves the noise immunity of estimates with respect to corrupted data in the observation matrix and has a rapid convergence. Despite the good results obtained, the statistical efficiency of the IDIM-IV

estimates is not addressed, the relationships that exist between the IDIM-IV approach and the approaches in automatic control are not emphasized and the controller is assumed to be known to the user.

The aim of this paper is twofold. First, we show how a prefiltering process inspired by RIVC identification can be introduced into the IDIM-IV identification algorithm for robot system identification, so establishing links between the robotic and the automatic control approaches to identification. The resulting IDIM-PIV method extends the work undertaken in Brunot et al. (2017), where the IDIM-IV residuals are statistically analysed, and in Janot et al. (2017), where the joint velocities and accelerations are estimated with a state space estimation technique. Secondly, the issue of identifying the IDIM model in the presence of an unknown controller is addressed by a parametric identification. Practical validation of this new algorithm is carried by experiments conducted on a six Degrees-Of-Freedom (DOF) industrial robot arm, Stäubli TX40.

The paper is organised as follows. The next section provides the background to robot system architecture, including the models, control laws and sensors used in the analysis and control of robot systems, as well as the notation used in such analysis. Section 3 summarizes the standard techniques for robot identification and the use of prefilters in IV algorithms. In the fourth section, the proposed prefiltering process and the method of controller identification are described. The results of experiments are summarized in Section 5; and finally, the concluding remarks are provided in Section 6.

2. Robot System Architecture

2.1. Robot Dynamic Models

The Inverse Dynamic Model (IDM) of a rigid robot with n moving links is the expression of the $(n \times 1)$ torque vector, $\boldsymbol{\tau}_{idm}$, as a function of the joint positions and their derivatives (Khalil and Dombre, 2004). The following relationship is derived by application of Newton's law or the Lagrangian equations:

$$\boldsymbol{\tau}_{idm}(t) = \boldsymbol{M}\left(\boldsymbol{q}_{nf}(t)\right)\ddot{\boldsymbol{q}}_{nf}(t) + \boldsymbol{N}\left(\boldsymbol{q}_{nf}(t), \dot{\boldsymbol{q}}_{nf}(t)\right) \tag{1}$$

where $\boldsymbol{M}$ is the $(n \times n)$ inertia matrix; $\boldsymbol{N}$ is the $(n \times 1)$ vector of centrifugal, Coriolis, gravitational, and friction torques; and $\boldsymbol{q}_{nf}$, $\dot{\boldsymbol{q}}_{nf}$, $\ddot{\boldsymbol{q}}_{nf}$ are, respectively, the $(n \times 1)$ noise-free vectors of joint positions, velocities and

accelerations. According to Gautier (1986), a joint j of an industrial robot has 14 standard parameters:

$$\boldsymbol{\chi}_j = [XX_j \quad XY_j \quad XZ_j \quad YY_j \quad YZ_j \quad ZZ_j \quad MX_j \quad MY_j \quad MZ_j \quad M_j \quad Ia_j \quad F_{v_j} \quad F_{c_j} \quad \tau_{off_j}]^T \tag{2}$$

where XX_j, XY_j, XZ_j, YY_j, YZ_j and ZZ_j are the six components of the inertia matrix at the origin of frame j; MX_j, MY_j, MZ_j are the three components of the first moments; M_j is the mass of link j; Ia_j is the total inertia moment for rotor and gears of the actuator; F_{v_j} and F_{c_j} are, respectively, the viscous and Coulomb friction coefficients; τ_{off_j} is an offset parameter containing the asymmetry of the Coulomb friction with respect to the sign of the velocity and the current amplifier offset which supplies the motor.

Since some of these parameters have no effect on the dynamic model, while others are regrouped with linear relations, we obtain a $(b \times 1)$ vector of base dynamic parameters: $\boldsymbol{\theta}$; see (Gautier, 1991). In addition, the IDM is linear with respect to the base parameters and so we obtain the following linear relation

$$\boldsymbol{\tau}_{idm}(t) = \boldsymbol{\phi}\left(\boldsymbol{q}_{nf}(t), \dot{\boldsymbol{q}}_{nf}(t), \ddot{\boldsymbol{q}}_{nf}(t)\right)\boldsymbol{\theta} = \boldsymbol{\phi}_{nf}(t)\boldsymbol{\theta}, \tag{3}$$

where $\boldsymbol{\phi}$ is the $(n \times b)$ matrix of basis functions (from hereon referred to as the 'observation matrix'). It is worth noting that base parameters are simply referred to as model parameters in Marconato et al. (2013). Each element of $\boldsymbol{\phi}$ is a basis function of the body dynamics. These basis functions can be nonlinear relationships involving the positions, velocities and accelerations and the nature of these nonlinearities can be estimated, if this is required, using the approach suggested in Janot et al. (2017).

As a result of inevitable measurement noise and modelling errors, the actual torque $\boldsymbol{\tau}$ differs from $\boldsymbol{\tau}_{idm}$ by an error $\boldsymbol{v}$, so that the usual definition of the Inverse Dynamic Identification Model (IDIM) is given by

$$\boldsymbol{\tau}(t) = \boldsymbol{\tau}_{idm}(t) + \boldsymbol{v}(t) = \boldsymbol{\phi}\left(\boldsymbol{q}_{nf}(t), \dot{\boldsymbol{q}}_{nf}(t), \ddot{\boldsymbol{q}}_{nf}(t)\right)\boldsymbol{\theta} + \boldsymbol{v}(t). \tag{4}$$

The associated DDM relates the joint accelerations to a *nonlinear* function of the states (positions and velocities) and the parameters: e.g.,

$$\ddot{\boldsymbol{q}}_{nf}(t) = \boldsymbol{M}\left(\boldsymbol{q}_{nf}(t)\right)^{-1}\left(\boldsymbol{\tau}_{idm}(t) - \boldsymbol{N}\left(\boldsymbol{q}_{nf}(t), \dot{\boldsymbol{q}}_{nf}(t)\right)\right). \tag{5}$$

2.2. Control Laws

As pointed out previously, robots need to operate within a closed-loop control system due to their double integrator behaviour. In particular, the joint positions are controlled within two nested loops: an inner-loop for the current control and an outer-loop for the position control. Most often the control laws are simple Proportional Derivative (PD), Proportional Integral Derivative (PID), or computed torque and passive control (see Chapter 14 in Khalil and Dombre, 2004, for details on this topic). In the present paper, it is assumed that the controller is linear; that each link is controlled separately from the others; and that there is one position sensor (i.e. an encoder or a resolver) for each link. This is a typical configuration for an industrial robot, as explained in Khalil and Dombre (2004). According to the same reference, the integral action is usually weak, or even deactivated when the position error is too small, in order to avoid oscillations due to the Coulomb friction.

Considering the link j, the controller C_j is defined by

$$\nu_{\tau_j}(t) = C_j(p)(q_{r_j}(t) - q_{m_j}(t)), \tag{6}$$

where C_j denotes the controller (normally a PD or PID in practice), $p = d/dt$ is the differential operator, ν_{τ_j} is the control signal, q_{r_j} is the reference trajectory and q_{m_j} is the measured position. For convenience, the controller is modelled as a continuous-time system although, in practice, it is implemented in Discrete Time (DT) on the micro-controllers that are used to perform the control actions. The control signal, ν_{τ_j}, serves as a reference to the inner current loop of the amplifiers that supply the motors. Assuming that the current closed-loop has a bandwidth greater than 500 Hz, its transfer function is modelled as a static gain, g_{τ_j} that applies in the frequency range of the rigid robot dynamics ω_{dyn} (usually less than 10 Hz). The actual torque of the link τ_j is then calculated by

$$\tau_j(t) = g_{\tau_j}\nu_{\tau_j}(t). \tag{7}$$

2.3. Position Sensor

The $(n \times 1)$ vector of measured joint positions can be expressed as

$$\boldsymbol{q}_m(t) = \boldsymbol{q}(t) + \boldsymbol{\xi}(t), \tag{8}$$

where $\boldsymbol{q}$ is the $(n \times 1)$ vector of joint positions and $\boldsymbol{\xi}$ is a $(n \times 1)$ vector of continuous-time noises source. In order to avoid problems associated

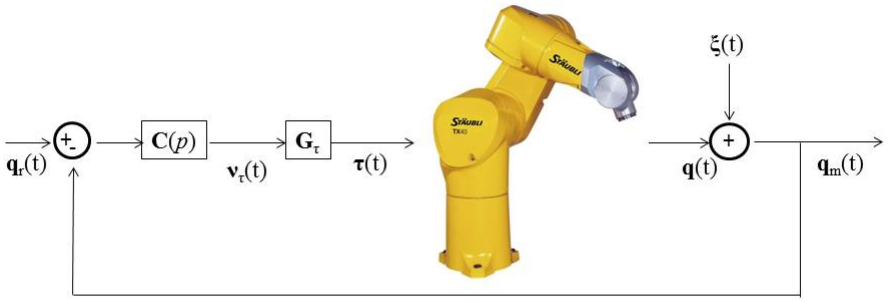

Figure 1: Closed-loop diagram of Stäubli TX40 robot

with continuous-time white noise inputs, the noise filters are considered as discrete-time systems (see e.g. Gilson et al., 2008; Young, 2015, and the prior references therein). Consequently, the output noise is given by

$$\boldsymbol{q}_m(t_i) = \boldsymbol{q}(t_i) + \boldsymbol{\xi}(t_i) = \boldsymbol{q}(t_i) + \boldsymbol{H}(z^{-1})\boldsymbol{e}(t_i), \qquad i = 1, \cdots n_m \tag{9}$$

where $\boldsymbol{H}$ is the $(n \times n)$ output noise transfer function matrix in the backward shift (delay) operator z^{-1}, i.e. $z^{-1}e(t) = e(t - \Delta t)$, where Δt is the sampling interval; $\boldsymbol{e}$ is a $(n \times 1)$ vector of zero mean value, white noise inputs with $(n \times n)$ covariance matrix $\boldsymbol{\Lambda}$; and n_m is the number of recorded measurements. By including the modelling elements, Figure 1 illustrates the closed-loop structure of the robot considered in this study.

Since there is one independent sensor per link, $\boldsymbol{H}$ is set diagonal and composed of filters $H_j(z^{-1})$, $j = 1, 2, \ldots, n$. Furthermore, the white noise elements in the $(n \times 1)$ vector $\boldsymbol{e}$ are assumed to be uncorrelated and so the covariance matrix $\boldsymbol{\Lambda}$ is also diagonal, with a covariance λ_j for the link j. Following from this, the equation for each link j takes the form

$$q_{m_j}(t_i) = q_j(t_i) + H_j(z^{-1})e_j(t_i). \tag{10}$$

According to Bélanger et al. (1998), a shaft encoder has a white, zero mean and uniformly distributed noise with a variance equal to $\frac{1}{3}\Delta^2$, where Δ is the encoder resolution. Swevers et al. (2007) have pointed out that, in a factory environment, the position sensors can be influenced by other machines like welding apparatus and other electromagnetic disturbances. For

this reason, we consider a more general case where the noise is not necessary white, especially at high frequency. A covariance proportional to Δ^2 seems reasonable in the operating range of system, i.e. below ω_{dyn}.

According to Marcassus et al. (2007), the resolution of the Stäubli TX40 robot is 2×10^{-4} degree per count. Such a resolution is common for an industrial robot that needs to respect the standard (ISO, 1998), with criteria on position accuracy and repeatability, amongst others (see e.g. Khalil and Dombre, 2004). This order of magnitude shows that the spectral density of the noise is really low below ω_{dyn}. Consequently, the measurement noise $H_j(z^{-1})e_j(t_i)$, of link j, is assumed to have a spectral density located in high frequencies and that this spectral density can vary.

2.4. Closed-loop Relations

In order to highlight the role of the filters used for the standard IDIM-LS and IDIM-IV methods, as summarized later in Section 3, we now need to consider the closed-loop system in more detail by examining the situation at joint j. The linear part of the DDM, $G_j(p)$, is defined by

$$G_j(p) = \frac{1}{p(J_j p + F_{v_j})}, \tag{11}$$

namely a free integrator in series with a first order system, where F_{v_j} the viscous friction coefficient and J_j given by

$$J_j = \max_{\boldsymbol{q}_{nf}}(\boldsymbol{M}_{jj}(\boldsymbol{q}_{nf})). \tag{12}$$

J_j is the maximum value, with respect to $\boldsymbol{q}_{nf}$, of the inertia moment and this defines the smallest stability margin of the position closed-loop as $\boldsymbol{q}_{nf}$ varies. The joint j can be modelled as shown in Figure 2, where d_j is the nonlinear disturbance regrouping the Coulomb friction, the centrifugal, Coriolis, gravitational torques and the coupling effects, such as

$$d_j(t) = -N_j\left(\boldsymbol{q}_{nf}(t), \dot{\boldsymbol{q}}_{nf}(t)\right) + F_{v_j}\dot{q}_{nf_j}(t) - \sum_{k=1,k\neq j}^{n} M_{jk}(\boldsymbol{q}_{nf}(t))\ddot{q}_{nf_k}(t) \tag{13}$$

with N_j, the j^{th} element of $\boldsymbol{N}$ defined by (1). The whole system is modelled as a hybrid one: the dynamic system and the controller models are continuous time, whereas the noise filter is discrete time. Although the robot system

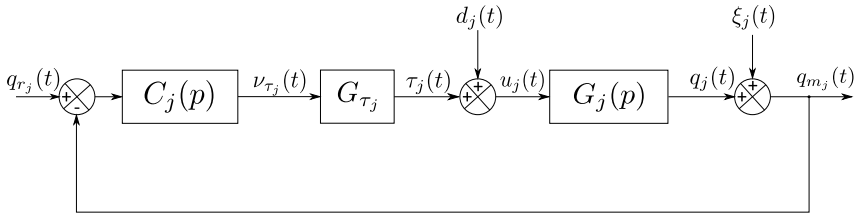

Figure 2: Robot model of link j

operates in closed-loop, the identification concerns the open-loop dynamic model from the input command signal ν_{τ_j} and output position signal q_{m_j}.

From Figure 2, the following closed-loop relationships can be derived,

$$\begin{aligned} q_{m_j}(t) &= T_j(p)q_{r_j}(t) + S_j(p)\xi_j(t) + S_j(p)G_j(p)d_j(t) \\ T_j(p) &= \frac{g_{\tau_j}C_j(p)G_j(p)}{1 + g_{\tau_j}C_j(p)G_j(p)}, \quad S_j(p) = \frac{1}{1 + g_{\tau_j}C_j(p)G_j(p)} \end{aligned} \tag{14}$$

where S_j is the sensitivity function and T_j is the complementary sensitivity function: see e.g. Aström and Murray (2010). As explained in the previous section, a discrete time model is more suitable for the noise filter representation. Therefore, the closed-loop relation can re-written informally in hybrid terms

$$q_{m_j}(t_i) = T_j(p)q_{r_j}(t_i) + S_j(p)H_j(z^{-1})e_j(t_i) + S_j(p)G_j(p)d_j(t_i). \tag{15}$$

Since for each p, $T_j(p) + S_j(p) = 1$, both functions cannot be made small simultaneously. In order to have a good tracking at low frequencies, the controller is tuned to insure $T_j(p) \approx 1$ and, consequently, $S_j(p) \approx 0$. As T_j is a low-pass filter, we have the opposite configuration at high frequencies. Noting that the relevant information comes from the reference signal, the closed-loop transfer function T_j provides an ideal frequency range for the filtering process. In this range, we have $T_j(p) \approx 1$, $S_j(p) \approx 0$ and the component from the noise becomes negligible. For these reasons, it is sensible to filter the measured position close to the closed-loop dynamics in order to retrieve a low noise position signal. Note that this is consistent with Chapter 14 in Khalil and Dombre (2004), which suggests that PID control laws provide good tracking if there are high position gains and the integral action is weak.

Finally, the closed-loop transfer function of the position, q_j, is given by

$$q_j(t_i) = T_j(p)q_{r_j}(t_i) - T_j(p)H_j(z^{-1})e_j(t_i) + S_j(p)G_j(p)d_j(t_i), \tag{16}$$

while the torque closed-loop transfer function is defined by

$$\tau_j(t_i) = g_{\tau_j} C_j(p) S_j(p) \left[q_{r_j}(t_i) - H_j(z^{-1}) e_j(t_i) \right] - T_j(p) d_j(t_i). \qquad (17)$$

3. Closed-loop System Identification

The purpose of the identification process is here to provide a reliable model for the design of control laws. In the robotic context, continuous-time design is the norm. Therefore, the identified model is continuous-time; i.e. the parameters are not a function of the sampling interval. In practice, this model can be digitised to any appropriate sampling interval for digital control implementation.

3.1. The IDIM-LS Method

The LS regression method is the most straightforward method for IDIM model parameter estimation because the IDIM is linear with respect to the parameters. However, for this to be applied without introducing asymptotic bias on the estimates, the IDIM model formulation requires the regressors in the measurement vector to be adequately filtered in order to deal with any noise on the measured robot data.

The Bandpass Filtering Process

In most applications, the available information is the $(n \times 1)$ measurement vector of the joint positions, $\boldsymbol{q}_m$. The joint velocities and accelerations have to be retrieved from this information in order to build the observation matrix $\boldsymbol{\phi}$, as described in Gautier (1997). First, $\boldsymbol{q}_m$ is filtered to obtain an estimate $\widehat{\boldsymbol{q}}$ and then, if this filtering is adequate, the derivatives can be calculated using centralized finite differencing, while limiting noise amplification. In order to achieve this objective, the filter type and the cut-off frequency, ω_{f_q}, are selected such that $\left(\widehat{\boldsymbol{q}}, \widehat{\dot{\boldsymbol{q}}}, \widehat{\ddot{\boldsymbol{q}}}\right) \approx (\boldsymbol{q}_{nf}, \dot{\boldsymbol{q}}_{nf}, \ddot{\boldsymbol{q}}_{nf})$ in the range $[0, \omega_{f_q}]$. The filter, which is usually of the Butterworth two-pass or 'smoothing' variety (filtfilt routine in Matlab$^{\text{TM}}$), where it is applied in both forward and reverse directions to eliminate the phase lag that is inherent in the forward-pass filtering operation. The signals are obtained in this manner because they are then used to construct the nonlinear basis functions, operations that do not tolerate the presence of any phase distortion in the component signals. The rule of thumb for the cut-off frequency is $\omega_{f_q} \geq 5\omega_{dyn}$, which is consistent with the observations made in relation to equation (15). The combination

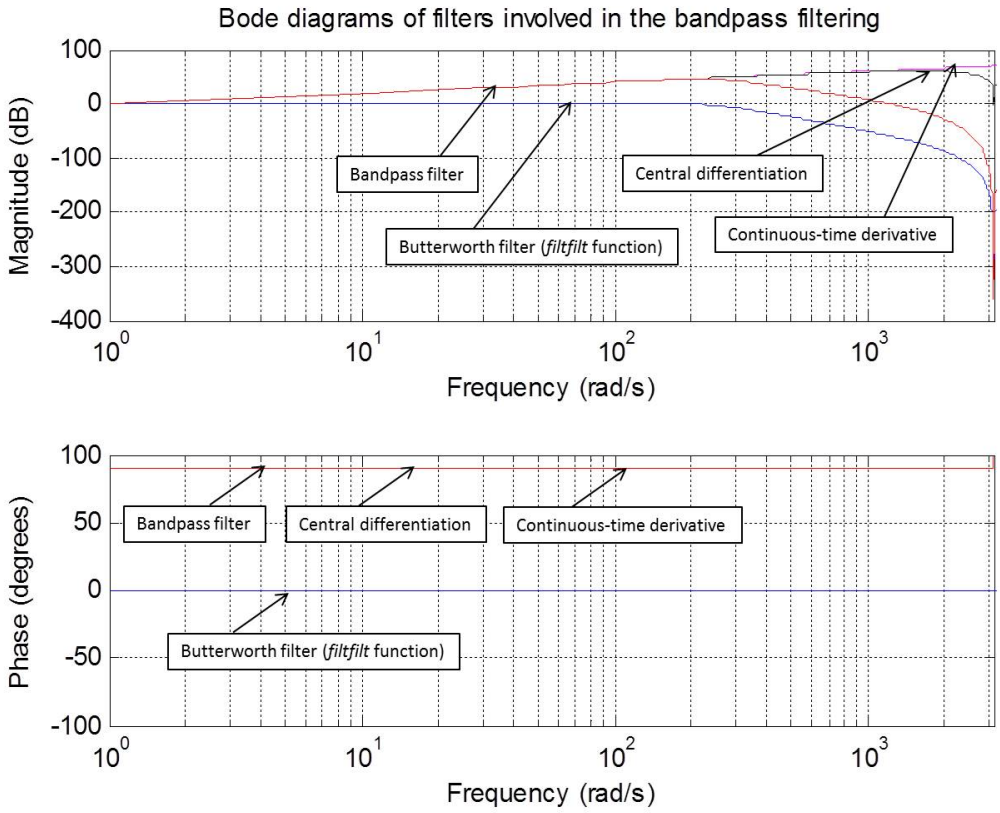

Figure 3: Bode diagram of filters involved in the bandpass filtering

of the two-pass Butterworth filter and central differencing is referred to as the *BandPass* (BP) filtering process. Figure 3 depicts the tuning of this BP filtering for a system with a Nyquist frequency of 1 kHz and a robot bandwidth of 10 Hz. Consequently the Butterworth filter cut-off frequency is tuned to 50 Hz. As expected, the bandpass filter behaves like the continuous-time differentiation in the robot's bandwidth and rejects the high frequency components.

In practice, the torque is perturbed by high-frequency ripples: unmodelled friction and flexibility effects, which are rejected by the controller. These ripples are removed prior to the identification with a parallel lowpass filtering of each basis function at the cut-off frequency $\omega_{F_p} \geq 2\omega_{dyn}$. As shown in equation (17) of Section 2.4, the choice of ω_{F_p} may be invoked to retain enough information, while attenuating the high frequency noise. Since there

is no more useful information beyond the cut-off frequency, the parallel low-pass filtering is used as part of a 'decimation' procedure: i.e. resampling to keep one sample over $n_d = \omega_{nyq}/\omega_{Fp}$. After data acquisition and decimation, we obtain

$$\boldsymbol{\tau}_{F_p}(t_i) = F_p(z^{-1})\boldsymbol{\tau}(t_i) = \boldsymbol{\phi}_{F_p}\left(\widehat{\boldsymbol{q}}(t_i), \widehat{\dot{\boldsymbol{q}}}(t_i), \widehat{\ddot{\boldsymbol{q}}}(t_i)\right)\boldsymbol{\theta} + \boldsymbol{v}_{F_p}(t_i), \qquad (18)$$

with F_p the parallel filter applied to each element of the observation matrix $\boldsymbol{\phi}_{F_p}\left(\widehat{\boldsymbol{q}}(t_i), \widehat{\dot{\boldsymbol{q}}}(t_i), \widehat{\ddot{\boldsymbol{q}}}(t_i)\right) = F_p(z^{-1})\boldsymbol{\phi}\left(\widehat{\boldsymbol{q}}(t_i), \widehat{\dot{\boldsymbol{q}}}(t_i), \widehat{\ddot{\boldsymbol{q}}}(t_i)\right)$, as well as the error vector $\boldsymbol{v}_{F_p}(t_i) = F_p(z^{-1})\boldsymbol{v}(t_i)$.

Least-Squares

If n_m measurements are recorded during the experiment, after the re-sampling we have $N = n_m/n_d$ available sets of data. From (18), there is an overdetermined linear system which can be solved using standard LS regression analysis: i.e.,

$$\widehat{\boldsymbol{\theta}}_{LS}(N) = \left[\frac{1}{N}\sum_{i=1}^{N}\boldsymbol{\phi}_{F_p}^T(t_{(i)})\boldsymbol{\phi}_{F_p}(t_{(i)})\right]^{-1}\left[\frac{1}{N}\sum_{i=1}^{N}\boldsymbol{\phi}_{F_p}^T(t_{(i)})\boldsymbol{\tau}_{F_p}(t_{(i)})\right], \qquad (19)$$

with $t_{(i)} = t_{i.n_d} = t_0 + i.n_d/f_m$, where t_0 and f_m are, respectively, the initial time and the recording frequency. Without modelling errors, the LS estimator is statistically consistent and efficient under the two conditions:

- $\bar{E}\left[\boldsymbol{\phi}_{F_p}^T(t)\boldsymbol{\phi}_{F_p}(t)\right]$ is full column rank;
- $\bar{E}\left[\boldsymbol{\phi}_{F_p}^T(t)\boldsymbol{v}_{F_p}(t)\right] = 0.$

where $\bar{E}[f(t)] = \lim_{N\to\infty}\frac{1}{N}\sum_{i=1}^{N}E[f(t_i)]$, with E the mathematical expectation (see e.g. Ljung, 1999). It is well known that, for closed-loop systems, the assumption that the observation matrix is not correlated with the error is not valid due to the feedback (see e.g. Van den Hof, 1998). This is clearly emphasized by comparing (15) and (17) where both q_{m_j} and τ_j are corrupted by e_j. In practice, however, *thanks to the appropriate filtering*, the IDIM-LS estimates remain statistically consistent, *provided that* ω_{f_q} *and* ω_{F_p} *are tuned accordingly to* Δ *and* ω_{dyn}.

3.2. Refined Instrumental Variable Identification

Another well-known technique for linear dynamic system estimation is the Instrumental Variable (IV) method, which is suitable for system identification in open or closed-loop situations. The standard IV approach is useful but can suffer from low statistical efficiency (high variance estimation). There is an approach to improving IV estimation in this regard: the one used in the present paper that exploits the notion of 'prefiltering' the data and is developed in the context of Maximum Likelihood (ML) estimation (see Young, 2015, and the prior references therein).

The Refined IV (RIV) estimation algorithm is an iterative method that jointly estimates the system and noise parameters of a Box-Jenkins model. Young (2015) shows how the RIV iterative algorithms are based on the ML formulation and can be considered either as a special Gauss-Newton procedure, or as a simple application of Pseudo-Linear Regression (PLR) (see Solo, 1980). The RIV estimate is given by

$$\widehat{\boldsymbol{\theta}}_{RIV}(N) = \left[\frac{1}{N}\sum_{i=1}^{N}\boldsymbol{\zeta}^T(t_i)\boldsymbol{L}(z^{-1})\boldsymbol{\phi}(t_i)\right]^{-1}\left[\frac{1}{N}\sum_{i=1}^{N}\boldsymbol{\zeta}^T(t_i)\boldsymbol{L}(z^{-1})\boldsymbol{\tau}(t_i)\right]. \tag{20}$$

Here $\boldsymbol{\zeta}$ is the $(n\times b)$ instrumental matrix and $\boldsymbol{L}$ is a $(n\times n)$ matrix of optimal prefilters. If there are no modelling errors, the RIV estimate is consistent under the two conditions required for IV estimation, namely:

- $\bar{E}\left[\boldsymbol{\zeta}^T(t)\boldsymbol{\phi}_{\boldsymbol{L}}(t)\right]$ is full column rank;
- $\bar{E}\left[\boldsymbol{\zeta}^T(t)\boldsymbol{v}_{\boldsymbol{L}}(t)\right] = 0.$

The first condition means that the instrumental matrix must be well correlated with the observations (termed *instrument relevance* by Wooldridge, 2008). The second condition expresses the fact that the instrumental matrix must be uncorrelated with the noise on the observations and is sometimes referred to as the *instrument exogeneity*.

In the present context, assuming no modelling error, the observational noise vector $\boldsymbol{v}$ in (4) is assumed to be modelled as follows

$$\boldsymbol{v}(t_i) = \boldsymbol{H}_\tau(z^{-1})\boldsymbol{e}(t_i), \tag{21}$$

where $\boldsymbol{e}$ is a $(n\times 1)$ white noise vector, with zero mean and $(n\times n)$ covariance matrix $\boldsymbol{\Lambda}$; and $\boldsymbol{H}_\tau$ is a $(n \times n)$ discrete-time transfer function matrix, the

elements of which are assumed to be asymptotically stable and invertible. Section 4.1 provides further information about this noise model.

RIV theory shows that the optimal variance is reached with

$$\boldsymbol{L}(z^{-1}) = \boldsymbol{\Lambda}^{-1}\boldsymbol{H}_{\tau}^{-1}(z^{-1}) \qquad \boldsymbol{\zeta}(t_i) = \boldsymbol{L}(z^{-1})\boldsymbol{\phi}_{nf}(t_i). \tag{22}$$

while the optimal covariance matrix (i.e. the lower bound) is given by

$$\boldsymbol{P}^{opt} = \left\{ \bar{E}\left[\left[\boldsymbol{H}_{\tau}^{-1}(z^{-1})\boldsymbol{\phi}_{nf}(t_i)\right]^T \boldsymbol{\Lambda}^{-1} \left[\boldsymbol{H}_{\tau}^{-1}(z^{-1})\boldsymbol{\phi}_{nf}(t_i)\right]\right]\right\}^{-1}. \tag{23}$$

The main question raised by this general formulation of the problem is the choice of the instruments to estimate $\boldsymbol{\phi}_{nf}$. This has received a lot of attention in automatic control, (see e.g. Söderström and Stoica, 1983, and the references given previously in the introduction) and section 4 below considers the prefiltered IV method we propose for use in robot identification.

3.3. The IDIM-IV Method

In the context of robot model identification, Janot et al. (2014b) have shown that the simulation of the DDM provides a very convenient way to obtain the instruments. This simulation model contains the whole closed-loop and, following previous IV terminology, is referred to as the 'auxiliary model' (Levadi, 1964). From the simulation of this auxiliary model, noise-free simulated signals are retrieved and used to construct the instrumental matrix. These signals are noise-free since the only input is the reference trajectory which is perfectly known. By noting the simulated signals with a subscript s, the instrumental matrix is defined as $\boldsymbol{\zeta}(t_i) = F_p(z^{-1})\boldsymbol{\phi}\left(\boldsymbol{q}_s(t_i), \dot{\boldsymbol{q}}_s(t_i), \ddot{\boldsymbol{q}}_s(t_i)\right)$, which can be viewed as an estimation of the noise-free part of the observation matrix.

The IDIM-IV method (Janot et al., 2014b) includes the parallel filter and the downsampling process, i.e. $\boldsymbol{L}(z^{-1}) \leftarrow F_p(z^{-1})\boldsymbol{I}_n$, with $\boldsymbol{I}_n$ the $(n \times n)$ identity matrix. This has the advantage of being more robust to inappropriate filtering than the IDIM-LS method, as shown in Janot et al. (2014b); and since it is a valid IV estimator, the IDIM-IV estimates are statistically consistent, so that

$$\boldsymbol{\epsilon}_{\boldsymbol{\tau}}(t) = \boldsymbol{\tau}(t) - \boldsymbol{\Phi}\left(\widehat{\boldsymbol{q}}(t), \widehat{\dot{\boldsymbol{q}}}(t), \widehat{\ddot{\boldsymbol{q}}}(t)\right)\widehat{\boldsymbol{\theta}}, \tag{24}$$

is also a consistent estimation of $\boldsymbol{v}(t)$ (White, 1980; Janot et al., 2014b).

The main limitation of the IDIM-IV method is that it does not take into account the noise model $\boldsymbol{H}_\tau(z^{-1})$ in (21). The first objective in this paper is, therefore, to remove this limitation and so generate estimates with reduced variance and improved statistical efficiency arising for the introduction of special prefilters. This yields the IDIM-Prefiltered IV (IDIM-PIV) algorithm, which is developed in the next section 4.

4. Prefiltered Instrumental Variable Identification for Robot Systems

Many IV techniques have been suggested in the automatic control and systems literature to identify common model structures, such as AutoRegressive Moving Average with eXogenous inputs (ARMAX) or Box-Jenkins (BJ) models (see e.g. Gilson et al., 2011). The IDIM-PIV method is inspired by the Refined IV (RIV) family of methods for estimating the parameters in discrete or continuous-time LTI transfer function models.

The special nature of the RIVC algorithm lies in the nature of the prefilter, which is hybrid in form and optimal in the sense that the algorithm yields maximum likelihood parameter estimates for LTI models that have minimum variance, i.e. the estimates achieve the Cramer-Rao lower variance bound (see section 3.2). In the following sub-section 4.1, we consider a related prefilter, inspired by the RIVC prefilter, that can be used within a closed loop setting for robot identification. However, because of the nonlinear nature of the dynamic system and the functions involved in the observation matrix, neither the prefilter nor the estimates can be considered necessarily as fully optimal in this sense although, as we shall see, they do lead to estimates that have smaller variance than those of the standard IDIM-IV.

4.1. Input Noise Model

The model of the closed loop feedback system for link j of the robot system, as depicted by Figure 2, has similarities with the closed loop systems considered in (Gilson et al., 2008) and chapter 9 of (Young, 2011). However, the two methods described in these references cannot be applied in a straightforward way in the present robotic context. This is because the robot identification variable is the input torque, τ_j, and not the output position; and the disturbance, d_j, is function of the states (position and velocity) and the user has no influence on this.

In order to highlight the torque noise, it is best to consider the controller equation for link j which, from (6), (7) and (9), takes the form:

$$\begin{aligned}\tau_j(t_i) &= g_{\tau_j} C_j(p)(q_{r_j}(t_i) - q_{m_j}(t_i)) \\ &= g_{\tau_j} C_j(p)(q_{r_j}(t_i) - q_j(t_i)) - g_{\tau_j} C_j(p) H_j(z^{-1}) e_j(t_i) \\ &= \boldsymbol{\phi}_j\left(\boldsymbol{q}(t_i), \dot{\boldsymbol{q}}(t_i), \ddot{\boldsymbol{q}}(t_i)\right)\boldsymbol{\theta} - g_{\tau_j} C_j(p) H_j(z^{-1}) e_j(t_i) \\ &= \boldsymbol{\phi}_j\left(\boldsymbol{q}(t_i), \dot{\boldsymbol{q}}(t_i), \ddot{\boldsymbol{q}}(t_i)\right)\boldsymbol{\theta} + H_{\tau_j}(z^{-1}) e_j(t_i),\end{aligned} \tag{25}$$

where $\boldsymbol{\phi}_j$ is the j^{th} row of the observation matrix $\boldsymbol{\phi}$ and the signals q_{r_j}, q_{m_j} and q_j are defined in Figure 2. Combining continuous and discrete-time operators informally, in order to illustrate the hybrid nature of the problem, we see that,

$$H_{\tau_j}(z^{-1}) = -g_{\tau_j} C_j(p) H_j(z^{-1}) \tag{26}$$

The objective is then to use H_{τ_j} as a prefilter for the PIV method.

4.2. The Integrated Random Walk Smoother

The standard BP method for estimating the joint velocities and accelerations is suboptimal and requires *a priori* knowledge of the system bandwidth. An optimal and fully automatic alternative method that does not require such knowledge is based on a combination of the Kalman Filter and Fixed Interval Smoother (KF-FIS). This is described in chapter 4 of Young (2011), which provides a full description of the general approach applied to a variety of different state-space model forms. This approach was first suggested for off-line differentiation of signals in the identification of continuous-time linear and nonlinear systems by Young et al. (1993); and was later applied to continuous-time nonlinear engineering systems by Coca and Billings (1999). This same approach can be used in the present robot identification context by modelling the joint position j as a simple Integrated Random Walk (IRW) process described by a simple state equation of the form,

$$\begin{aligned}\begin{bmatrix} q_j(t_i) \\ \dot{q}_j(t_i) \end{bmatrix} &= \begin{bmatrix} 1 & \Delta t \\ 0 & 1 \end{bmatrix} \begin{bmatrix} q_j(t_{i-1}) \\ \dot{q}_j(t_{i-1}) \end{bmatrix} + \begin{bmatrix} 0 \\ 1 \end{bmatrix} \varpi_j(t_{i-1}), \\ q_{m_j}(t_i) &= q_j(t_i) + \xi_j(t_i),\end{aligned} \tag{27}$$

where ϖ_j and ξ_j are, respectively, the process and measurement noise inputs; q_j and $\dot{q}_j$ are the states to be estimated; Δt is the fixed sampling period and a single hyper-parameter, in the form of the Noise Variance Ratio (NVR) associated with the stochastic input $\varpi_j(t_i)$, is optimised by maximum likelihood

based on 'prediction error decomposition' (see e.g Harvey and Peters, 1990). The resulting KF-FIS algorithm yields the estimates $\widehat{q}_j$ and $\widehat{\dot{q}}_j$ that are required to construct the observation matrix. This Integrated Random Walk SMoothing (IRWSM) algorithm is coded as the routine irwsm in the CAPTAIN Toolbox[1] for Matlab™ and, by applying this simple routine twice, the joint acceleration estimate can be retrieved. It should be stressed that, thanks to the maximum likelihood optimisation, the practitioner does not have to provide any priori knowledge. Recently, Janot et al. (2017) have introduced this as an alternative to the conventional bandpass filtering process.

Finally, note that it is important not to confuse this KF-FIS *filtering* procedure, nor the standard BP filtering operations that it replaces, with the *prefiltering* used in the IDIM-PIV algorithm, since these fulfill quite different filtering objectives. The term 'prefiltering' is restricted to the iteratively updated prefiltering used in the IDIM-PIV algorithm described in the next section 4.3,.

4.3. Main IDIM-PIV Identification Algorithm

In the IDIM-PIV algorithm, we introduce the $(l_j \times 1)$ vector of noise parameters $\boldsymbol{\eta}_j$ for link j. The $(l \times 1)$ noise vector $\boldsymbol{\eta}$ then regroups all these noise parameters, with $l = \sum_{j=1}^{n} l_j$ and $\boldsymbol{\eta}^T = [\boldsymbol{\eta}_1^T \dots \boldsymbol{\eta}_n^T]$. Finally, the complete set of parameters required for IDIM-PIV estimation are stacked in the $(b+l \times 1)$ vector $\boldsymbol{\rho}^T = [\boldsymbol{\theta}^T \quad \boldsymbol{\eta}^T]$. With n_m sample points, the algorithm is then defined by the following iterative process:

1. **Initialisation**. For the initial physical parameters, $\widehat{\boldsymbol{\theta}}^0$, use the Computer-Aided Design (CAD) values for the inertia, with the other physical parameters are set to zero. For each link, the initial noise filter is set as follows: $H_j(z^{-1}, \widehat{\boldsymbol{\eta}}_j^{\,0}) = 1$ with $\widehat{\lambda}_j^0 = 1$. If the controller is known then move to step 2. If the controller is unknown, it must be identified first using the approach described in Section 4.5. The observation matrix is constructed using the IRWSM algorithm.

2. **Iteration**: repeat the following steps until convergence is achieved, where k indicates the k^{th} iteration:

[1] This Toolbox is available free and can be downloaded via http://captaintoolbox.co.uk.

(a) Simulate the auxiliary model (i.e. the DDM), using the previous estimated parameter vector $\widehat{\boldsymbol{\theta}}^{k-1}$, in order to retrieve the noise-free signals for the instruments.

(b) Compute the IDIM-PIV estimate of the physical parameters using the following IV solution, where the prefiltering is accomplished using the noise model from the previous iteration:

$$\widehat{\boldsymbol{\theta}}^{k} = \left[\sum_{i=1}^{n_m}\sum_{j=1}^{n} \boldsymbol{\zeta}_j^T(t_i,\widehat{\boldsymbol{\rho}}^{k-1})\boldsymbol{\phi}_{L_j}(t_i,\widehat{\boldsymbol{\rho}}^{k-1})\right]^{-1}\left[\sum_{i=1}^{n_m}\sum_{j=1}^{n} \boldsymbol{\zeta}_j^T(t_i,\widehat{\boldsymbol{\rho}}^{k-1})\tau_{L_j}(t_i,\widehat{\boldsymbol{\rho}}^{k-1})\right] \tag{28}$$

with

$$\begin{aligned}
\boldsymbol{\phi}_{Lj}(t_i,\widehat{\boldsymbol{\rho}}^{k-1}) &= L_j(z^{-1},\widehat{\boldsymbol{\eta}}_j^{k-1})\boldsymbol{\phi}_j\left(\widehat{\boldsymbol{q}}(t_i),\widehat{\dot{\boldsymbol{q}}}(t_i),\widehat{\ddot{\boldsymbol{q}}}(t_i)\right),\\
\boldsymbol{\zeta}_j(t_i,\widehat{\boldsymbol{\rho}}^{k-1}) &= L_j(z^{-1},\widehat{\boldsymbol{\eta}}_j^{k-1})\boldsymbol{\phi}_j\left(\boldsymbol{q}_s(t_i,\widehat{\boldsymbol{\theta}}^{k-1}),\dot{\boldsymbol{q}}_s(t_i,\widehat{\boldsymbol{\theta}}^{k-1}),\ddot{\boldsymbol{q}}_s(t_i,\widehat{\boldsymbol{\theta}}^{k-1})\right),\\
\tau_{Lj}(t_i,\widehat{\boldsymbol{\rho}}^{k-1}) &= L_j(z^{-1},\widehat{\boldsymbol{\eta}}_j^{k-1})\tau_j(t_i),\\
L_j(z^{-1},\widehat{\boldsymbol{\eta}}_j^{k-1}) &= \left(\widehat{\lambda}_j^{k-1}\right)^{-1} H_{\tau_j}^{-1}(z^{-1},\widehat{\boldsymbol{\eta}}_j^{k-1}).
\end{aligned}$$

(c) For each link j, obtain an estimate of the noise parameters, $\widehat{\boldsymbol{\eta}}_j^k$, and an estimate of the noise covariance, $\widehat{\lambda}_j^k$. The output noise filter H_j can be identified based on

$$-g_{\tau_j}^{-1}C_j^{-1}(p)\epsilon_{\tau_j}(t_i) = H_j(z^{-1},\boldsymbol{\eta}_j)e_j(t_i), \tag{29}$$

with

$$\epsilon_{\tau_j}(t) = \tau_j(t) - \boldsymbol{\phi}_j\left(\widehat{\boldsymbol{q}}(t),\widehat{\dot{\boldsymbol{q}}}(t),\widehat{\ddot{\boldsymbol{q}}}(t)\right)\widehat{\boldsymbol{\theta}}^{k}. \tag{30}$$

The noise model, H_{τ_j}, is then reconstructed with (26).

3. **Estimated covariance**. After convergence, an approximate estimate of the parametric error covariance matrix, based on (23), is computed by the following relation

$$\boldsymbol{P}(\widehat{\boldsymbol{\theta}}) = \left\{\bar{E}\left[\sum_{j=1}^{n}\left[H_{\tau_j}^{-1}(z^{-1},\widehat{\boldsymbol{\eta}}_j)\boldsymbol{\phi}_j\left(t,\widehat{\boldsymbol{\theta}}\right)\right]^T\widehat{\lambda}_j^{-1}\left[H_{\tau_j}^{-1}(z^{-1},\widehat{\boldsymbol{\eta}}_j)\boldsymbol{\phi}_j\left(t,\widehat{\boldsymbol{\theta}}\right)\right]\right]\right\}^{-1}. \tag{31}$$

4.4. Noise Filter Identification

In general terms, an AutoRegressive, Moving Average (ARMA) model is used to represent the noise process H_{τ_j} in the IDIM-PIV algorithm, under the assumption that the noise has rational spectral density; and this model can be estimated by any available ARMA noise model identification method (e.g. the routine ivarma in CAPTAIN). However, an easier alternative, as used here, is to employ the simpler AutoRegressive (AR) model, with its order identified by the Akaike Information Criterion (AIC); as implemented by the aic routine in CAPTAIN. This simple method of noise model identification, combined with the irwsm approach to signal differentiation, means that IDIM-PIV algorithm does not require any access to prior information and so it is easier to apply in practice.

4.5. Controller Identification

When the controller is unknown, one solution is to use the IDIM-LS method, which does not require any knowledge on the controller. However, as shown in Janot et al. (2014b), it is more interesting to consider the IDIM-IV method if the system bandwidth is not certain. This is most likely to be the situation when first identifying a particular robotic system. The drawback of this approach is, of course, that the IDIM-IV method requires the controller knowledge for the simulation of the DDM, so it is necessary to use an alternative strategy.

If the controller structure is known to the practitioner, a parametric identification method provides a straightforward solution. If the structure is unknown, the control law (model and parameters) can be identified using standard techniques, such as RIV or Prediction Error Minimisation (PEM: see Ljung, 1999). In the robotic context, the controller inputs $\boldsymbol{q}_r$, $\widehat{\boldsymbol{q}}$, $\widehat{\dot{\boldsymbol{q}}}$ and $\widehat{\ddot{\boldsymbol{q}}}$, as well as its output: $\boldsymbol{\nu}_\tau$ are available. This poses a Multiple Input Single Output (MISO) problem of system identification, which can be identified by the method that best suits the practitioner (see e.g. Pascu et al. (2016)).

Finally, as Khalil and Dombre (2004) explain, a predictive/feed-forward action can be employed in robotic systems in order to reduce the tracking error. In this situation, therefore, it may well be relevant to take into account $\dot{\boldsymbol{q}}_r$ and $\ddot{\boldsymbol{q}}_r$ as additional inputs for the control law identification. Furthermore, since many industrial robots also have a velocity loop, the velocity $\widehat{\dot{\boldsymbol{q}}}$ can be a valuable input for the controller identification.

5. Experimental Results

5.1. Experimental Setup

The experimental evaluation of the proposed IDIM-PIV identification method has been carried out using the industrial Stäubli TX40 robot, which is a serial manipulator composed of six rotational joints; see Figure 1. There is a coupling between the joints 5 and 6 that adds two parameters: fv_{m6} and fc_{m6}, which are, respectively, the viscous and dry friction coefficient of the motor 6. The SYMORO+ software is used to automatically calculate the customized symbolic expressions of models (see Khalil and Dombre, 2004). The robot has 60 base dynamic parameters and, from these 60 base parameters, only 28 are well identified with good relative standard deviations. These 28 parameters define a set of essential parameters that are sufficient to describe the dynamic behaviour of the robot. This set was validated with a F-statistic, as shown in Janot et al. (2014a) and only the estimation of these parameters is considered here.

The reference trajectories are trapezoidal velocities (also called smoothed bang-bang accelerations) that lead to the signals shown in Figure A.9. With $cond(\boldsymbol{\phi}_{F_p}) = 200$, these reference trajectories provide sufficient excitation for the estimation of the base parameters according to Gautier and Khalil (1991)[2]. The joint positions and control signals are stored with a measurement frequency $f_m = 5$ kHz. For the IDIM-LS method, the filter cut-off frequencies are tuned according to Gautier et al. (2013a): i.e. $\omega_{f_q} = 5\omega_{dyn} = 50$ Hz and $\omega_{F_p} = 2\omega_{dyn} = 20$ Hz for the Butterworth and the decimation filters, respectively. The maximum bandwidth for joint 6 is $\omega_{dyn} = 10$ Hz. Concerning the control law, a simple controller has been designed to perform tests in the laboratory. This controller is composed of one PID per axis and is referred to as the 'actual controller'.

The identification is conducted using rather noisy data in order to test the performance of the methods in this regard. For this purpose, the resolution of the encoders is downgraded to 3600 points per revolution in an equivalent manner to Marcassus et al. (2007). The order of the AR noise model is selected using the aic routine in CAPTAIN, which makes the procedure automatic but identifies very high order models in this case. This suggests

[2]Given the IV nature of the estimation, $cond(\boldsymbol{\zeta}^T\boldsymbol{\phi}_{F_p})$ should also be checked as this will ensure that the instrumental variables are well generated and the IV solution is well defined.

that the noise is complex, which probably arises from artifacts introduced in the decimation and filtering operations required in the preparation of the data for model identification. However, the resulting prefilter is able to purge the colour satisfactorily from the noise on data and, as we shall see, produces a worthwhile improvement in the residual autocorrelations and reduction in the estimation error variance.

5.2. Known Controller

Three identification methods are considered in this case: the proposed IDIM-PIV; the standard IDIM-LS; and the IDIM-IV without prefilters. For the IDIM-IV and IDIM-PIV methods, the controller used for the simulation is the actual controller of the robot. The observation matrix for the IDIM-PIV method is constructed automatically using the CAPTAIN irwsm implementation of the IRWSM algorithm; while the usual bandpass filter design approach is used for the other methods.

For continuous-time modelling purposes, the Coulomb friction is modelled with a *arctangent* function instead of a *sign* function (see Gautier et al., 2013b). The function $\frac{2}{\pi}atan(\gamma\dot{q}_j(t))$ tends to $sign(\dot{q}_j(t))$ when γ tends to infinity but, in the present situation a $\gamma = 150$ appeared to be satisfactory and avoided any numerical integration problems. It is worth noting here that the prior assumption of known relationships for nonlinearities such as this is not essential because they can be estimated using the State-Dependent Parameter (SDP) approach discussed in Janot et al. (2017).

Table 1 summarizes the estimated values and their relative standard deviations. The estimated parameters of the IDIM-LS method are not satisfactory due to large mismatches in the estimated inertias zz_{1_r} and zz_{3_r}: this is the result of estimation bias induced by the noise correlation arising from closed-loop operation. The IDIM-IV and IDIM-PIV methods converged in 3 and 5 iterations, respectively, and the resulting estimated parameters were checked using cross-validation tests in an equivalent manner to Janot et al. (2014a). In practice, the experimental dataset was divided in two: the first part for the identification and the second one for the cross-validation. Figures 4 and A.7 show a comparison between actual joint torques (blue) and reconstructed joint torques (dashed red). The reconstructed torques, based on the IDIM-PIV estimates, fit the actual ones as well as the reconstructed ones based on the standard IDIM-IV method.

With regard to the relative standard deviations, except for two parameters (fv_2 and zz_{3_r}), the values are less than those of the IDIM-IV method, and

Table 1: Estimated parameters and relative standard deviations

Param.	IDIM-LS	IDIM-IV	IDIM-PIV	IDIM-PIV ($\widehat{C}$)
zz_{1_r}	**1.12** (2.43%)	1.24 (2.64%)	1.25 (1.20%)	1.25 (1.17%)
fv_1	8.06 (1.23%)	7.61 (1.45%)	7.61 (1.12%)	7.61 (1.09%)
fc_1	6.94 (3.95%)	8.34 (3.74%)	8.33 (2.89%)	8.32 (2.82%)
xx_{2_r}	-0.43 (5.45%)	-0.46 (6.30%)	-0.46 (4.34%)	-0.46 (4.25%)
xz_{2_r}	-0.15 (7.87%)	-0.16 (10.6%)	-0.16 (8.71%)	-0.16 (8.52%)
zz_{2_r}	0.97 (1.94%)	1.13 (2.05%)	1.13 (1.70%)	1.14 (1.64%)
mx_{2_r}	2.44 (3.72%)	2.25 (5.84%)	2.16 (1.66%)	2.16 (1.62%)
fv_2	5.59 (1.93%)	5.11 (2.38%)	5.19 (2.48%)	5.20 (2.41%)
fc_2	7.94 (3.09%)	9.23 (3.00%)	8.99 (3.22%)	8.97 (3.13%)
xx_{3_r}	0.16 (13.8%)	0.14 (18.2%)	0.12 (16.2%)	0.12 (15.8%)
zz_{3_r}	**-0.01** (265%)	0.11 (18.2%)	0.14 (10.9%)	0.14 (10.3%)
my_{3_r}	-0.61 (4.20%)	-0.61 (4.77%)	-0.56 (4.50%)	-0.56 (4.39%)
ia_3	0.16 (8.68%)	0.09 (18.5%)	0.09 (11.2%)	0.09 (11.0%)
fv_3	2.06 (3.59%)	1.77 (4.62%)	1.71 (4.12%)	1.72 (3.98%)
fc_3	5.88 (4.21%)	7.23 (3.83%)	7.60 (3.07%)	7.59 (2.98%)
mx_4	0.00 (272%)	-0.03 (50.2%)	-0.07 (16.5%)	-0.07 (15.2%)
ia_4	0.02 (39.6%)	0.03 (28.8%)	0.03 (18.0%)	0.03 (16.8%)
fv_4	1.20 (6.21%)	0.97 (8.37%)	0.85 (4.26%)	0.85 (4.18%)
fc_4	2.13 (12.6%)	3.13 (9.49%)	3.55 (3.68%)	3.53 (3.61%)
my_{5_r}	-0.05 (19.6%)	-0.04 (30.4%)	-0.03 (24.0%)	-0.02 (25.1%)
ia_5	0.05 (16.7%)	0.05 (24.5%)	0.05 (16.0%)	0.05 (14.7%)
fv_5	1.97 (4.80%)	1.55 (6.68%)	1.60 (4.13%)	1.60 (3.73%)
fc_5	2.43 (10.1%)	3.82 (7.16%)	3.71 (4.66%)	3.75 (4.14%)
ia_6	0.01 (40.7%)	0.01 (64.5%)	0.01 (20.5%)	0.01 (21.1%)
fv_6	0.68 (6.79%)	0.59 (8.84%)	0.59 (3.96%)	0.60 (3.53%)
fc_6	0.14 (146%)	0.19 (68.1%)	0.26 (59.3%)	0.26 (59.1%)
fv_{m6}	0.62 (5.91%)	0.53 (7.57%)	0.56 (3.99%)	0.56 (3.51%)
fc_{m6}	1.91 (11.0%)	2.35 (9.98%)	2.61 (4.97%)	2.46 (4.76%)

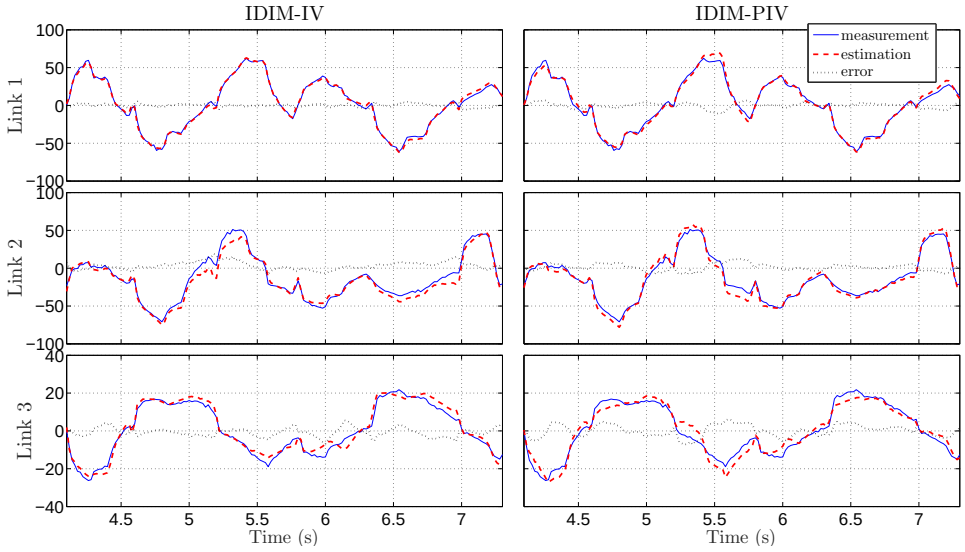

Figure 4: Cross-validation torques (Nm): measurement (blue), estimation (dashed red) and error (dotted black) – IDIM-IV (left) and IDIM-PIV (right) – Controller known – Axes 1 to 3

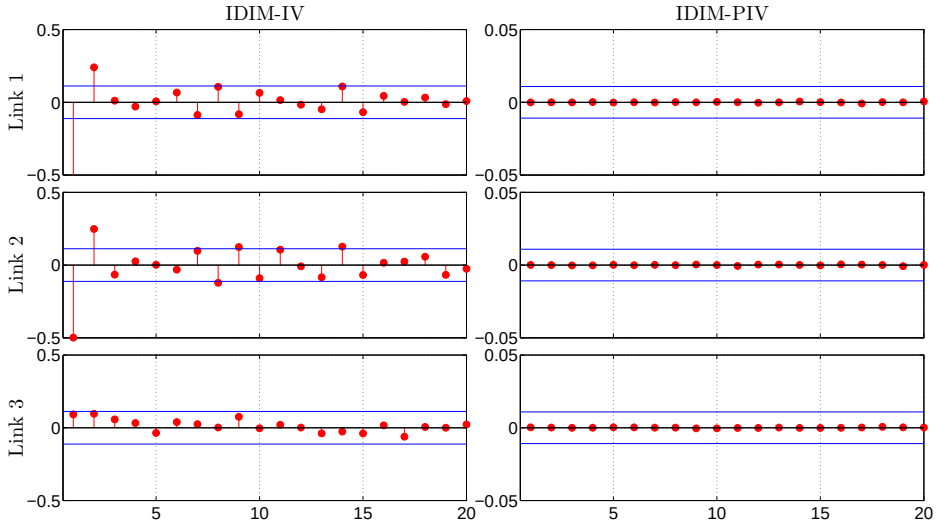

Figure 5: IDIM-IV (left) and IDIM-PIV (right) residuals autocorrelations (red dots) and 2σ confidence intervals (blue lines) – Controller known – Axes 1 to 3

sometimes significantly so, even though the filters of the latter are correctly tuned. The reason why there is no improvement in these two parameters is unclear but it may be because of the small remaining modeling error that affects the estimated noise signal and the estimation of the $H(z^{-1})$ which, as we note in section 5, require very high order AR models. Furthermore, the estimated covariances of the IDIM-PIV method seem more reliable, as we see clearly from Figures 5 and A.8 which show the autocorrelation functions of the model residuals obtained in each case. For the IDIM-PIV method, the effect of the prefilter is clear, with the estimated autocorrelation coefficients included well within the confidence intervals indicated by the blue lines; whereas they are larger for the IDIM-IV method and exceed the confidence intervals, so revealing significant serial autocorrelation. Note that the differences between the confidence interval bounds are due to the number of samples considered for each methods: the IDIM-PIV method uses $n_m = 34500$ sampling points for the estimation, while the others use only $N = n_m/n_d = 276$ sampling points, due to the need for the decimation filter.

Based on the above results, we can conclude that, when the controller is known, the IDIM-PIV method is able to estimate the robot parameters very well. Although the standard IDIM-IV method yields reasonable results, it is more sensitive to the noise contained in the signals, showing that the addition of the prefiltering in IDIM-PIV method is advantageous and provides a worthwhile improvement. Finally, the IDIM-LS method fails in this situation and has to be considered unsatisfactory in this regard.

5.3. Unknown Controller

When the controller is unknown, a parametric approach has been considered. This is used in the case in the IDIM-PIV algorithm, with the Simplified Refined IV (SRIV) option in the CAPTAIN rivcbj routine employed to identify a parametric model for the controller. The identified controller model is composed of six PID elements and is indicated by $\widehat{C}$. For link j, the input and the output of the corresponding PID controller are, respectively, the tracking error $(q_{r_j} - q_{m_j})$ and the control signal ν_{τ_j}. In addition, the velocity and acceleration of the reference, $\dot{q}_{r_j}$ and $\ddot{q}_{r_j}$ respectively, as well as the estimated velocity, $\widehat{q}_j$, were taken into account, so providing more flexibility to identify the control law. The user has to provide the routine with these signals, as well as the orders of the numerator and denominator of the transfer for the given link. In order to identify these orders, maximum orders are selected at first; then, a linear search is performed to select the orders that

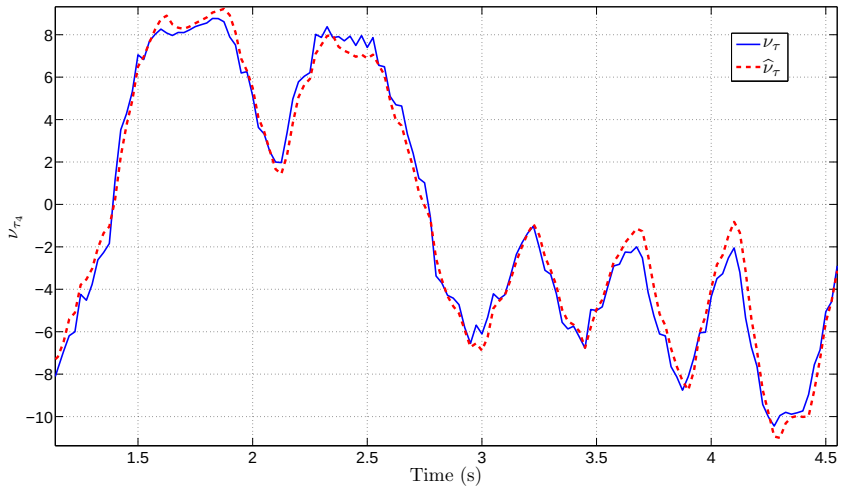

Figure 6: Example of the identification of the controller – Axis 4

give the best explanation of the data. Figure 6 shows the identified controller of link 4 as an example. As described in (Young, 2015), the SRIV option of the rivcbj routine estimates the continuous-time transfer function using an iterative RIV method under the assumption of white additive noise. In this case, the observation matrix for the IDIM-PIV method is again constructed using the CAPTAIN irwsm technique.

The IDIM-PIV method converged well in 5 iterations. Based on the identification results shown in the last column of Table 1, the IDIM-PIV method clearly shows that parametric identification of the controller provides an effective approach when the controller is unknown. Once again, the relative standard deviations of the IDIM-PIV estimates are slightly lower than those of the IDIM-IV method, demonstrating again the advantages of prefiltering.

6. Conclusions

Inspired by the optimal hybrid Refined Instrumental Variable algorithm for continuous time linear systems (RIVC), the existing IDIM-IV algorithm for nonlinear robotic system identification has been modified to a new IDIM-PIV form that includes iteratively updated prefilters to improve its statistical efficiency. The instrumental variables and prefilters are derived from the closed-loop model of the robot which is identified systematically, without *a*

priori knowledge of the system or, if necessary, the associated control system. If the controller is unknown, the paper shows how it can be identified using a parametric method based on the RIVC algorithm.

Experimental validation of the proposed methodology has been carried out on a 6 DOF industrial robot and it is concluded that:

- The IDIM-PIV is suitable for the systematic identification of an industrial robot without access to the prior knowledge normally required for such identification;
- The observation matrix required by the IDIM-PIV algorithm can be automatically constructed using the Integrated Random Walk Smoothing (IRWSM) technique;
- If the control system is unknown *a priori*, then a suitable model for the controller can be identified using the existing RIVC parametric method;
- The controller identification strategies can be used with standard IDIM-IV technique, freeing it also from any prior knowledge in this regard.
- The RIVC and IRWSM algorithms required for implementation of the IDIM-PIV algorithm are available as the rivcbj and irwsm routines in the CAPTAIN Toolbox for Matlab™

Research and development studies are continuing on the IDIM-PIV approach, concentrating on its application to more flexible robots and/or parallel robots. In this regard, (Vivas et al., 2003), (Guegan et al., 2003), (Briot and Gautier, 2015)(Wu et al., 2010) have applied the standard IDIM-LS method to parallel robots; while in (Wu et al., 2008), the authors have applied a standard LS procedure that is equivalent to the IDIM-LS approach. These successful studies suggest that the IDIM-IV and the IDIM-PIV methods should be suitable also for parallel robot applications.

Appendix A. Supplementary figures

This appendix includes supplementary figures for the axes 4 to 6 as well as a plot of the excitation trajectories used for this study.

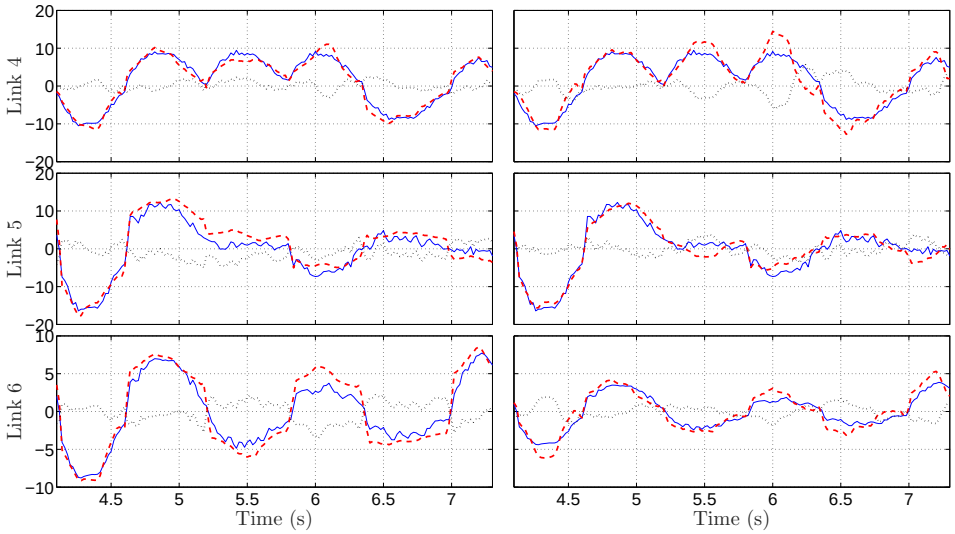

Figure A.7: Cross-validation torques (Nm): measurement (blue), estimation (dashed red) and error (dotted black) – IDIM-IV (left) and IDIM-PIV (right) – Controller known – Axes 4 to 6

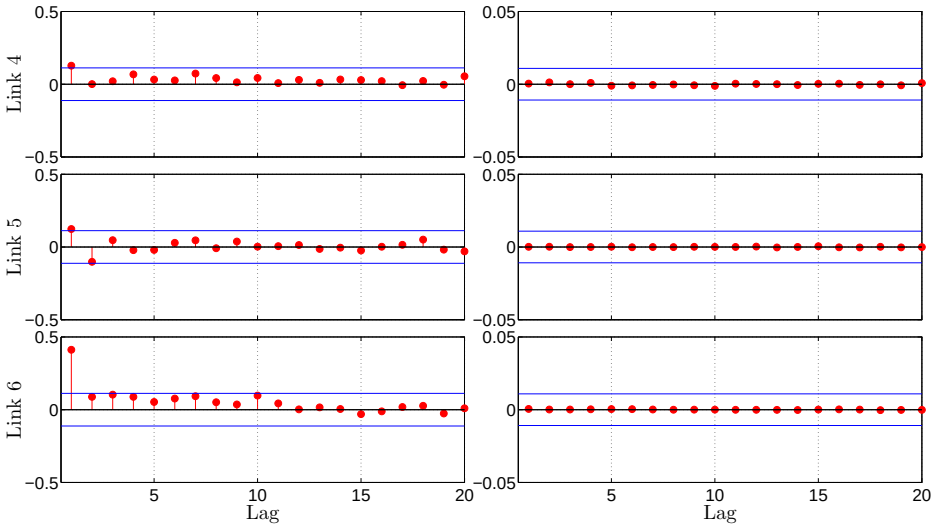

Figure A.8: IDIM-IV (left) and IDIM-PIV (right) residuals autocorrelations (red dots) and 2σ confidence intervals (blue lines) – Controller known – Axes 4 to 6

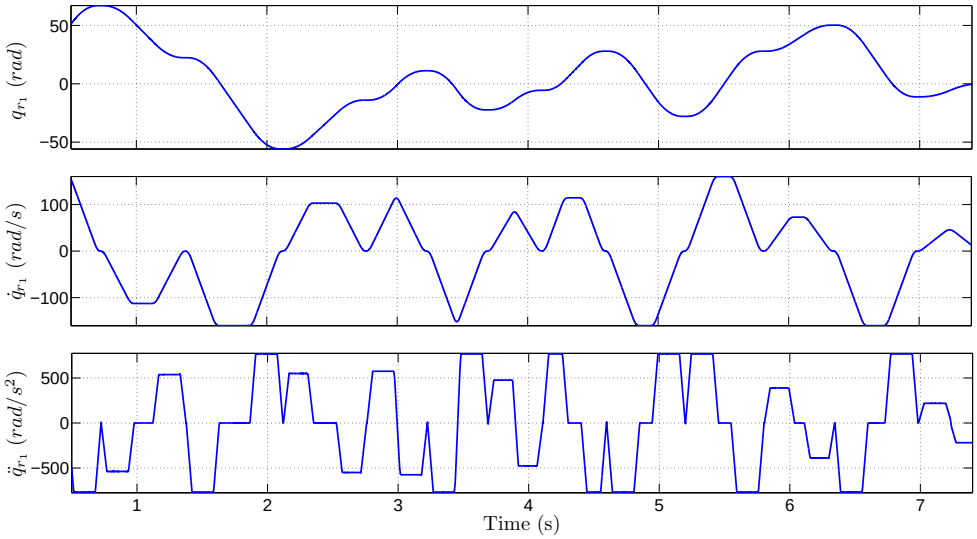

Figure A.9: Excitation trajetories example – Axis 1 – Position (top), velocity (middle) and acceleration (bottom)

References

Aström, K. J., Murray, R. M., 2010. Feedback systems: an introduction for scientists and engineers. Princeton university press.

Bélanger, P., Dobrovolny, P., Helmy, A., Zhang, X., 1998. Estimation of angular velocity and acceleration from shaft-encoder measurements. The International Journal of Robotics Research 17 (11), 1225–1233.

Briot, S., Gautier, M., 2015. Global identification of joint drive gains and dynamic parameters of parallel robots. Multibody System Dynamics 33 (1), 3–26.

Brunot, M., Janot, A., Carrillo, F., Garnier, H., July 2017. A pragmatic and systematic statistical analysis for identification of industrial robots. In: 2017 IEEE International Conference on Advanced Intelligent Mechatronics (AIM). pp. 559–564.

Calafiore, G. C., Indri, M., 1999. Identification of a robot dynamic model: experiment design and parameter estimation.

Calanca, A., Capisani, L. M., Ferrara, A., Magnani, L., 2011. Mimo closed loop identification of an industrial robot. IEEE Transactions on Control Systems Technology 19 (5), 1214–1224.

Coca, D., Billings, S. A., 1999. A direct approach to identification of nonlinear differential models from discrete data. Mechanical Systems and Signal Processing 13(5),, 739–755.

Dellon, B., Matsuoka, Y., 2009. Modeling and system identification of a life-size brake-actuated manipulator. IEEE Transactions on Robotics 25 (3), 481–491.

Dolinskỳ, K., Čelikovskỳ, S., 2017. Application of the method of maximum likelihood to identification of bipedal walking robots. IEEE Transactions on Control Systems Technology.

Gautier, M., 1986. Identification of robots dynamics. In: IFAC Symposium on Theory of Robots. Vienna, pp. 351—356.

Gautier, M., 1991. Numerical calculation of the base inertial parameters of robots. Journal of robotic systems 8 (4), 485–506.

Gautier, M., 1997. Dynamic identification of robots with power model. In: Robotics and Automation, 1997. Proceedings., 1997 IEEE International Conference on. Vol. 3. IEEE, pp. 1922–1927.

Gautier, M., Janot, A., Vandanjon, P.-O., 2013a. A new closed-loop output error method for parameter identification of robot dynamics. IEEE Transactions on Control Systems Technology 21 (2), 428–444.

Gautier, M., Jubien, A., Janot, A., 2013b. Iterative learning identification and computed torque control of robots. In: Intelligent Robots and Systems (IROS), 2013 IEEE/RSJ International Conference on. IEEE, pp. 3419–3424.

Gautier, M., Khalil, W., 1991. Exciting trajectories for the identification of base inertial parameters of robots. In: Proceedings of the 30th IEEE Conference on Decision and Control. pp. 494–499.

Gautier, M., Poignet, P., 2001. Extended kalman filtering and weighted least squares dynamic identification of robot. Control Engineering Practice 9 (12), 1361–1372.

Gilson, M., Garnier, H., Young, P. C., Van den Hof, P., 2008. Instrumental variable methods for closed-loop continuous-time model identification. In: Identification of continuous-time models from sampled data. Springer, pp. 133–160.

Gilson, M., Garnier, H., Young, P. C., Van den Hof, P. M., 2011. Optimal instrumental variable method for closed-loop identification. IET control theory & applications 5 (10), 1147–1154.

Guegan, S., Khalil, W., Lemoine, P., 2003. Identification of the dynamic parameters of the orthoglide. In: Robotics and Automation, 2003. Proceedings. ICRA'03. IEEE International Conference on. Vol. 3. IEEE, pp. 3272–3277.

Harvey, A. C., Peters, S., 1990. Estimation procedures for structural time series models. Journal of Forecasting 9 (2), 89–108.

Hollerbach, J., Nahvi, A., 1997. Total least squares in robot calibration. Experimental Robotics IV, 274–282.

ISO, E., 1998. 9283: 1998. Manipulating industrial robots-Performance criteria and related test methods.

Jakeman, A. J., Young, P. C., 1979. Refined instrumental variable methods of time-series analysis: Part II, multivariable systems. International Journal of Control 29, 621–644.

Janot, A., Vandanjon, P.-O., Gautier, M., 2014a. A generic instrumental variable approach for industrial robot identification. IEEE Transactions on Control Systems Technology 22 (1), 132–145.

Janot, A., Vandanjon, P. O., Gautier, M., 2014b. An instrumental variable approach for rigid industrial robots identification. Control Engineering Practice 25, 85–101.

Janot, A., Young, P. C., Gautier, M., 2017. Identification and control of electro-mechanical systems using state-dependent parameter estimation. International Journal of Control 90 (4), 643–660.

Khalil, W., Dombre, E., 2004. Modeling, identification and control of robots. Butterworth-Heinemann.

Khosla, P. K., Kanade, T., 1985. Parameter identification of robot dynamics. In: Decision and Control, 1985 24th IEEE Conference on. Vol. 24. IEEE, pp. 1754–1760.

Kostic, D., De Jager, B., Steinbuch, M., Hensen, R., 2004. Modeling and identification for high-performance robot control: An rrr-robotic arm case study. IEEE Transactions on Control Systems Technology 12 (6), 904–919.

Levadi, V. S., 1964. Parameter estimation of linear systems in the presence of noise. In: Proceedings, International Conference on Microwaves, Circuit theory and Information Theory, Tokyo.

Ljung, L., 1999. System identification: theory for the user. PTR Prentice Hall, Upper Saddle River, NJ.

Marcassus, N., Vandanjon, P.-O., Janot, A., Gautier, M., 2007. Minimal resolution needed for an accurate parametric identification-application to an industrial robot arm. In: 2007 IEEE/RSJ International Conference on Intelligent Robots and Systems. IEEE, pp. 2455–2460.

Marconato, A., Schoukens, M., Rolain, Y., Schoukens, J., 2013. Study of the effective number of parameters in nonlinear identification benchmarks. In: Decision and Control (CDC), 2013 IEEE 52nd Annual Conference on. IEEE, pp. 4308–4313.

Miranda-Colorado, R., Moreno-Valenzuela, J., 2017. An efficient on-line parameter identification algorithm for nonlinear servomechanisms with an algebraic technique for state estimation. Asian Journal of Control 19 (6), 2127–2142.

Olsen, M. M., Swevers, J., Verdonck, W., 2002. Maximum likelihood identification of a dynamic robot model: Implementation issues. The international Journal of robotics research 21 (2), 89–96.

Östring, M., Gunnarsson, S., Norrlöf, M., 2003. Closed-loop identification of an industrial robot containing flexibilities. Control Engineering Practice 11 (3), 291–300.

Pascu, V., Garnier, H., Ljung, L., Janot, A., 2016. Developments towards formalizing a benchmark for continuous-time model identification. In: Decision and Control (CDC), 2016 IEEE 55th Conference on. IEEE, pp. 7171–7176.

Puthenpura, S. C., Sinha, N. K., 1986. Identification of continuous-time systems using instrumental variables with application to an industrial robot. IEEE Transactions on Industrial Electronics (3), 224–229.

Ramdani, N., Poignet, P., 2005. Robust dynamic experimental identification of robots with set membership uncertainty. IEEE/ASME Transactions on Mechatronics 10 (2), 253–256.

Raucent, B., Campion, G., Bastin, G., Samin, J.-C., Willems, P. Y., 1992. Identification of the barycentric parameters of robot manipulators from external measurements. Automatica 28 (5), 1011–1016.

Reiersøl, O., 1941. Confluence analysis by means of lag moments and other methods of confluence analysis. Econometrica: Journal of the Econometric Society, 1–24.

Rowe, I. H., 1970. A bootstrap method for the statistical estimation of model parameters. International Journal of Control 12 (5), 721–738.

Söderström, T. D., Stoica, P. G., 1983. Instrumental variable methods for system identification. Vol. 57. Springer.

Soewandito, D. B., Oetomo, D., Ang, M. H., 2011. Neuro-adaptive motion control with velocity observer in operational space formulation. Robotics and Computer-Integrated Manufacturing 27 (4), 829–842.

Solo, V., 1980. Some aspects of recursive parameter estimation. Int. Jnl. Control 32, 395–410.

Swevers, J., Ganseman, C., Tukel, D. B., De Schutter, J., Van Brussel, H., 1997. Optimal robot excitation and identification. IEEE transactions on robotics and automation 13 (5), 730–740.

Swevers, J., Verdonck, W., De Schutter, J., 2007. Dynamic model identification for industrial robots. IEEE Control Systems 27 (5), 58–71.

Ting, J.-A., Mistry, M., Peters, J., Schaal, S., Nakanishi, J., 2006. A bayesian approach to nonlinear parameter identification for rigid body dynamics. In: Robotics: Science and Systems. pp. 32–39.

Van den Hof, P., 1998. Closed-loop issues in system identification. Annual reviews in control 22, 173–186.

Vivas, A., Poignet, P., Marquet, F., Pierrot, F., Gautier, M., 2003. Experimental dynamic identification of a fully parallel robot. In: Robotics and Automation, 2003. Proceedings. ICRA'03. IEEE International Conference on. Vol. 3. IEEE, pp. 3278–3283.

Wensing, P. M., Kim, S., Slotine, J.-J. E., 2018. Linear matrix inequalities for physically consistent inertial parameter identification: A statistical perspective on the mass distribution. IEEE Robotics and Automation Letters 3 (1), 60–67.

Wernholt, E., Gunnarsson, S., 2008. Estimation of nonlinear effects in frequency domain identification of industrial robots. IEEE Transactions on Instrumentation and Measurement 57 (4), 856–863.

White, H., 1980. A heteroskedasticity-consistent covariance matrix estimator and a direct test for heteroskedasticity. Econometrica: Journal of the Econometric Society, 817–838.

Wong, K., Polak, E., 1967. Identification of linear discrete time systems using the instrumental variable method. IEEE Transactions on Automatic Control 12 (6), 707–718.

Wooldridge, J., 2008. Introductory econometrics: A modern approach, 4th Edition. South-Western.

Wu, J., Wang, J., Wang, L., 2008. Identification of dynamic parameter of a 3dof parallel manipulator with actuation redundancy. Journal of Manufacturing Science and Engineering 130 (4), 041012.

Wu, J., Wang, J., You, Z., 2010. An overview of dynamic parameter identification of robots. Robotics and computer-integrated manufacturing 26 (5), 414–419.

Xi, F., 1995. Effect of non-geometric errors on manipulator inertial calibration. In: Robotics and Automation, 1995. Proceedings., 1995 IEEE International Conference on. Vol. 2. IEEE, pp. 1808–1813.

Yoshida, K., Ikeda, N., Mayeda, H., 1993. Experimental study of the identification methods for the industrial robot manipulator. Journal of the Robotics Society of Japan 11 (4), 564–573.

Young, P., 1976. Some observations on instrumental variable methods of time-series analysis. International Journal of Control 23 (5), 593–612.

Young, P., 1981. Parameter estimation for continuous-time models: a survey. Automatica 17 (1), 23–39.

Young, P., Foster, M., Lees, M., 1993. A direct approach to the identification and estimation of continuous-time systems from discrete-time data based on fixed interval smoothing. In: Proceedings, 12th Triennial IFAC World Congress on Automatic Control. Vol. 10. pp. 27–30.

Young, P. C., 1970. An instrumental variable method for real-time identification of a noisy process. Automatica 6 (2), 271–287.

Young, P. C., 2011. Recursive estimation and time-series analysis: an introduction for the student and practitioner, 2nd Edition. Springer Berlin Heidelberg.

Young, P. C., 2015. Refined instrumental variable estimation: Maximum likelihood optimization of a unified Box-Jenkins model. Automatica 52, 35–46.